Physicochem. Probl. Miner. Process., 61(5), 2025, 211192

http://www.journalssystem.com/mg/Lp

Physicochemical Problems of Mineral Processing

ISSN 1643-1049

Enhanced coarse particle flotation: A novel approach

Marly Carvalho [1,2], Ian Sherrel [3], Cagri Emer [4], Antti Rinne [1]

[1] Metso Finland Oy, Rauhalanpuisto 9, 02231, Espoo, Finland

[2] Oulu Mining School, Faculty of Technology, University of Oulu, FI-90014 Oulu, Finland

[3] Metso USA, 165 Shady Ln, Manchester, PA 17345

[4] Metso Maden Teknolojileri A.Ş, Macun Mah. 179. Sok. No:4/A, 06105, Ankara, Türkiye

Corresponding author: marly.carvalho@metso.com (Marly Carvalho)

Abstract: Size reduction is one of the most energy-intensive operations in mineral processing, often accounting for most of the energy consumption in a beneficiation plant. Despite its high energy demand, it is a necessary step to achieve adequate mineral liberation for traditional separation methods such as flotation. To reduce energy usage and improve process efficiency, alternative technologies are being developed to overcome the particle size limitations of conventional flotation equipment. A novel coarse particle flotation (CPF) device was designed to recover particles up to 1 mm in size, significantly extending the upper limit of conventional flotation, which typically operates effectively in the 20–150 μm range. The CPF device shares core operational principles with standard mechanical flotation cells but features a distinctive feed system that delivers the slurry directly into or onto the froth phase, enhancing the recovery of coarse particles while maintaining performance for fine particles. This study presents laboratory-scale results using the novel CPF cell applied in the grinding circuit with copper ore at P_{80}: 360 μm without feed classification to evaluate the effect of key operating variables, superficial gas velocity (Jg), froth depth, collector dosage, and frother concentration, on the performance of the CPF unit. The highest overall Cu recovery achieved was 89.6%, with 81.9% recovery in the +150 μm. These results were obtained without the use of fluidized water. The findings support the potential of this technology to improve coarse particle recovery and reduce energy consumption in modern flotation circuits.

Keywords: froth feeding, coarse particles flotation, base metals flotation

1. Introduction

Conventional froth flotation has been foundational in mineral processing for over a century and remains highly effective for concentrating particles within the 20–150 μm range (Clark et al., 2006; Mudd, 2009). Trahar and Warren (1976) published flotation data from copper, zinc, and lead flotation circuits showing the inefficiency of mechanical cells to float coarse and fine particles (Fig. 1). The inefficiency of conventional flotation for coarse particles has been linked to excessive energy dissipation via mechanical agitation, which weakens attachment forces and promotes detachment of bubble-particle aggregates and low retention time (Jameson, 2010; Wang et al., 2016; Hassanzadeh et al., 2022).

Absent a robust coarse flotation solution, the industry must grind all Run-of-Mine (ROM) ores to fine sizes suitable for conventional circuits, an energy-intensive and increasingly unsustainable practice (Awatey et al., 2015). Moreover, declining ore grades necessitate the processing of greater ROM volumes to sustain metal output, leading to heightened energy demands and bottlenecks in grinding circuits at brownfield operations (Mudd, 2009; Rötzer and Schmidt, 2020). Achieving separation at larger particle sizes offers a pathway to reject coarse gangue earlier in the circuit, thereby lowering energy usage or enhancing throughput during comminution.

Recent research has led to notable advancements in coarse particle flotation, focusing on enhanced hydrodynamics, improved bubble–particle interactions, and the development of hybrid flotation strategies (Anzoom et al., 2024). For example, studies on microbubble-assisted flotation in quartz benefi-

DOI: 10.37190/ppmp/211192

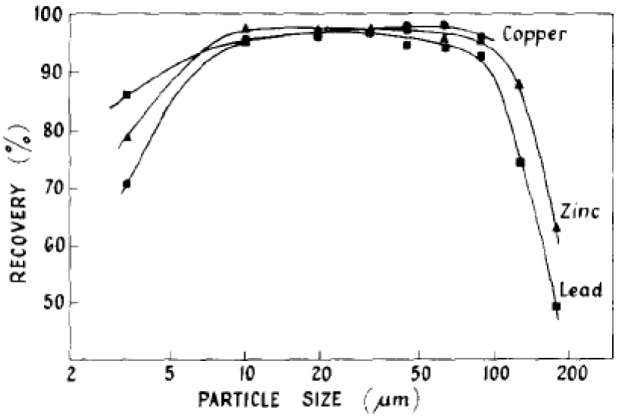

Fig. 1. Copper, zinc, and lead flotation recovery by particle size (Trahar and Warren, 1976)

ciation have demonstrated that microbubble presence significantly improves coarse particle recovery (Aslan and Abbaker, 2023). On the chemical front, new approaches such as targeted collector addition to bubble surfaces have shown promising improvements in coarse particle recovery (Forbes et al., 2025). Technological innovations include the integration of fluidization and air flotation, where upward liquid flow is used to suspend particles and promote attachment (Mankosa and Luttrell, 2002; Jameson, 2007; Jameson, 2010; Kromah et al., 2022).

Despite significant advances, coarse particle flotation by fluidized flotation cells still faces key operational challenges, including particle detachment and drop back, poor transfer efficiency from pulp to froth, and limited residence time or stability within the froth phase (Anzoom et al., 2024). Another constraint is their high-water demand for fluidization, which can be problematic in arid regions or sites with restricted water availability (Kromah et al., 2022). In particular, the HydroFloat™ separator operates with little or no froth layer and therefore requires pre-classification to remove fines before treatment, a limitation that reduces circuit flexibility (Kromah et al., 2022). Similarly, NovaCell™ demands careful control of cut-off velocities to maintain a stable bed while preventing ejection of larger particles, adding operational complexity during scale-up (Kromah et al., 2022). More broadly, fluidized-bed technologies require increasingly stringent fluidization control with coarser particle sizes, and they often necessitate tight feed classification and additional dewatering steps, which increase flowsheet complexity and cost (Jaques et al., 2021; Dankwah et al., 2022).

An alternative line of research has focused on the froth feeding principle, in which feed is introduced directly into the froth zone, thereby bypassing the turbulent slurry phase. This approach enhances the attachment of coarse particles to bubbles, minimizes detachment, and reduces their residence time in the pulp. Unlike fluidized-bed systems, froth feeding requires only the process water necessary for flotation, eliminating the need for additional fluidization water. According to the theoretical framework developed by Leppinen et al. (2003), the maximum floatable particle diameter under froth feeding conditions is promoted by flat or elongated particle geometries, high surface tension, and low particle density, whereas it is limited by high particle density and gravitational forces. Table 1 summarizes the estimated maximum floatable diameters for particles of different shapes and mineral types when applying the froth feeding method.

The froth feeding concept has been incorporated into several flotation devices over time. Knaus (1968) described its early form, where pre-aerated slurry spreads across the froth surface as aeration decreases. Ross (1993) advanced this with the DRL device, in which particles travel through a horizontal froth bed divided into concentrate, middlings, and tailings, stabilized by air sparging and a splitter plate. The SIF device by Nenno et al. (2004) introduced a funnel-shaped chamber, where bubble generation produces horizontal flow, enabling hydrophilic solids to settle while froth product is separately discharged. Uruzar (2011) further developed the idea with the FUD design, comprising a gas–pulp mixer followed by a froth tank to enhance bubble–particle contact and separation.

Building on this progression, Carvalho et al. (2025) and Tollander et al. (2025) introduced a novel coarse particle flotation (CPF) cell based on the froth feeding principle, which is evaluated in the present study. The cell incorporates several key innovations: a feed chamber with multiple slurry inlets and an

Table 1: Maximum floatable diameter (mm) with the froth feeding method. Adapted from Leppinen et al. (2003)

Mineral	Density (g/cm^3)	Cube A=4.82	Cylinder A=16/π	Sphere A=6	Octahedron A=10.4
Coal	1.55	3.40	3.50	3.80	5.00
Quartz	2.65	2.60	2.67	2.90	3.82
Diamond	3.50	2.26	2.33	1.52	3.32
Pyrite	5.20	1.86	1.91	2.07	2.73
Galena	7.65	1.53	1.57	1.71	2.25
Gold (metallic)	17.00	1.03	1.05	1.15	1.51

overflow weir that distributes feed uniformly across the froth, and a gas–liquid delivery system that injects water and bubbles into the cell while generating bubbles externally. Slurry is delivered directly into or onto the froth at low velocity in a pneumatic flotation configuration, thereby avoiding turbulence in the pulp zone. Unlike fluidization-based technologies, this design does not require additional fluidization water, yet it maintains compatibility with key flotation variables such as superficial gas velocity (Jg), frother and collector dosages, and froth depth. The CPF cell achieves product solids percentages similar to conventional TankCell® systems, allowing concentrate to be transferred directly to regrinding without dewatering, and it can process the full feed size distribution while still permitting optional pre-classification. Laboratory and pilot trials have consistently demonstrated high coarse particle recovery with this configuration, underscoring its potential as an alternative to existing CPF technologies. Fig. 2 illustrates the design of the CPF cell.

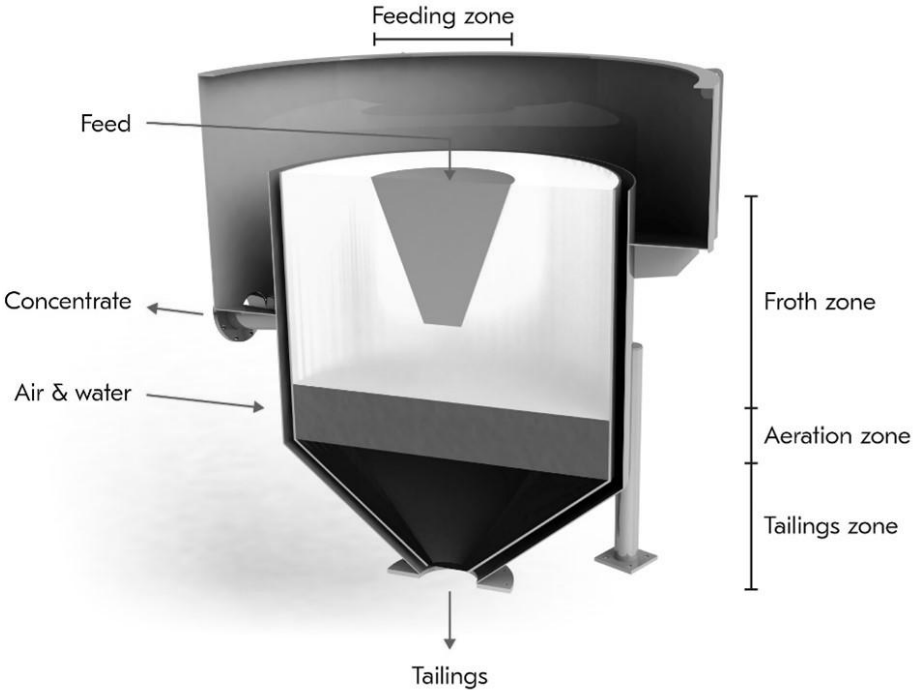

Fig. 2. CPF Cell

This study presents laboratory-scale results examining the effect of key process parameters on the performance of a novel coarse particle flotation (CPF) cell and illustrates its application in the grinding circuit, highlighting the main advantages, demonstrating its potential to improve coarse flotation efficiency in a manner that is scalable, energy-efficient, and economically sustainable. The research was conducted with the CPF cell integrated into the grinding circuit, illustrating its practical application within a copper processing flowsheet.

2. Materials and methods

2.1. Materials

The sample used in this study was a copper ore obtained from a mining site in South America, with the following composition: 0.83% Cu, 4.75% Fe, 53.60% SiO_2, and 0.081% S. Copper and iron concentrations were determined using Inductively Coupled Plasma Optical Emission Spectrometry (ICP-OES) after complete dissolution. The silicon dioxide (SiO_2) content was measured through colorimetric analysis using a Hach DR5000 UV-Vis spectrophotometer. Furthermore, the acid-soluble copper content was determined to be 0.08% Cu.

The analyzed sample was the feed ore from the beneficiation mill. Laboratory grindability tests were carried out to achieve a ground product with a P80 of 180 μm (standard particle size distribution), reflecting the plant's processed material. A second target with a P80 of 360 μm (coarser PSD) was prepared for flotation tests evaluating Metso's advanced coarse particle flotation technology. Fig. 3 presents the complete particle size distribution for both standard and coarse PSDs.

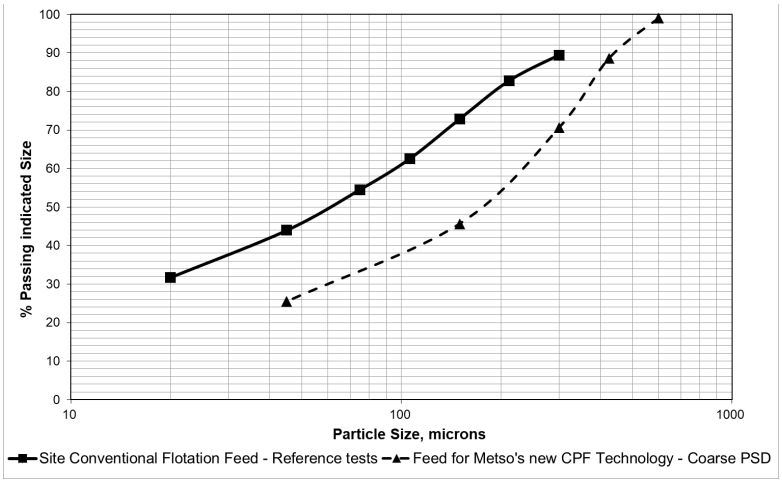

Fig. 3. Particle size distribution tested

2.2. Technologies tested and reagents

This study utilized two flotation devices: Metso's standard mechanical laboratory cell (GTK Labcell) for conventional flotation and reference tests, and a novel laboratory cell designed by Metso targeted to improve coarse particles flotation, CPF cell.

The reagent dosages were among the variables in the tests with the coarse particles flotation cell. Potassium Amyl Xanthate (PAX) was used as the collector in all tested technologies; however, a frother solution containing methyl isobutyl carbinol (MIBC) and DowFroth 250 (DF250) (at a 6:1 ratio) was applied in the reference tests with the conventional flotation cell, simulating the conditions on site. Flotanol C07 was tested as an alternative frother in the tests with the novel coarse particles flotation cell. The PAX dosages evaluated were 20 and 40 g/Mg, while the Flotanol C07 was tested at concentrations of 20 and 40 mg/dm^3.

2.3. Methodology

The tested sample underwent mineralogical characterization on resin-embedded sections examined under an optical microscope (Zeiss Axioplan 2, reflected light). Additional analyses were performed on carbon-coated polished sections using a JEOL-JSM 7000 field emission scanning electron microscope (FEG-SEM) equipped with an Oxford Instruments energy dispersive spectrometer (EDS) and integrated with Oxford Instruments' AZtec Mineral software for mineral liberation analysis.

Two reference tests were performed with the GTK lab cell with P80: 180 μm, and 11 tests with the novel coarse particles flotation cell at P80: 360 μm. During the grinding process, 12 g/Mg of PAX (collector) was conditioned in the mill. For the tests completed with the GTK lab cell, once grinding was

completed, the slurry was transferred to a 2 dm^3 bench-scale cell, and for the tests performed with the novel coarse particles flotation cell, the slurry was transferred to a conditioning tank. For the reference tests with the conventional flotation, another 12 g/Mg of PAX at pH 10 was conditioned for 1 min followed by the addition of 19 g/Mg of the frother solution with MIBC+DF250, and air was applied at a rate of 2 dm^3/min. The GTK lab cell was equipped with an automatic scraper system set to a 4-second cycle. After 7 min of flotation, an additional 8 g/Mg of PAX was added, conditioned for another minute, followed by the addition of 13 g/Mg of MIBC+DF250 solution. After this last stage of conditioning, the flotation continued for another 10 min. Each test resulted in one concentrate and one tailings sample, which were analyzed bulk. The methodology and conditions applied in the reference tests simulated the site. In the novel coarse particles flotation cell, 8 tests were part of a half-factorial Design of Experiments (DoE) planned with Minitab; 1 test was a repetition of a condition from the half-factorial tests, and 2 tests were carried out with fixed and optimized conditions aimed at maximizing copper recovery and the mass rejected to tailings. The slurry, combined with at least 10 kg of ore and water to achieve approximately 65% solids (w/w), was conditioned in a conditioning tank, while the froth was generated in the novel flotation cell. After conditioning, the cell was fed continuously on top of the froth until the conditioning tank was emptied. Although the setup is on a laboratory scale, it operates as a continuous single-pass unit throughout the duration of the test. For the tests conducted with the CPF flotation cell, the same collector used on-site was applied, but the tests were carried out with a stronger frother, Flotanol C07. Fig. 4 illustrates the flowsheet of the experimental program, and Table 2 provides a summary of the test conditions for each experiment. All samples produced during the tests with the novel coarse particles flotation cell were analyzed bulk and fractions of plus and minus 150 µm.

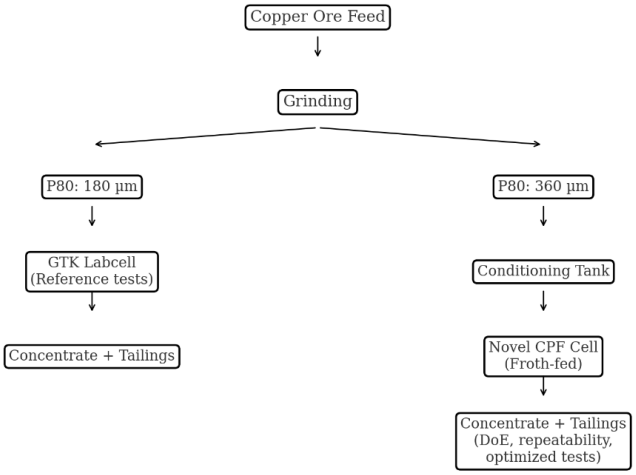

Fig. 4. Flowsheet of the experimental program

Table 2. Summary of tests performed with Metso's coarse particles flotation lab cell

Run Order	Collector Dosage (g/Mg)	Frother (mg/dm^3)	Froth Level (mm)	Jg (cm/s)	Note
1	20	20	250	2	1/2 Factorial
2	20	20	100	1	1/2 Factorial
3	20	40	250	1	1/2 Factorial
4	20	40	100	2	1/2 Factorial
5	40	20	250	1	1/2 Factorial
6	40	40	250	2	1/2 Factorial
7	40	40	100	1	1/2 Factorial
8	40	20	100	2	1/2 Factorial
9	40	40	250	2	Rep Test 6
10	40	40	400	2	Optimized Condition
11	40	40	400	2	Optimized Condition Rep

3. Results and discussion

3.1. Mineralogical characterization

The primary copper sulfide identified was chalcopyrite, with secondary sulfides such as chalcocite, covellite, and bornite. Pyrite was the dominant sulfide gangue mineral. Gangue phases included albite, amphiboles, calcite, chlorite, K-feldspar, magnetite, muscovite, and quartz. Notable mineral associations included chalcopyrite–bornite and chalcocite–covellite–bornite.

Liberation analysis of primary copper sulfides was performed on three particle size fractions: 425–600 µm, 300–425 µm, and 150–300 µm (Fig. 5). In the coarsest fraction, 26.7% of Cu-sulfides were liberated, 26.6% were locked within gangue, and the remainder occurred as high or low middlings. Liberation improved with decreasing size: 39.1% at 300–425 µm and 51.5% at 150–300 µm. The proportion of locked and middling grains decreased accordingly, indicating better flotation potential in finer fractions.

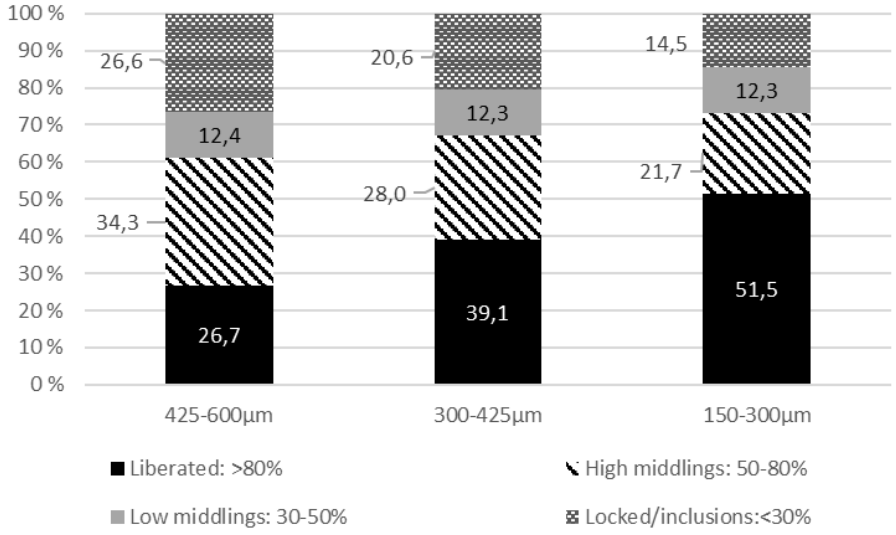

Fig. 5. Liberation of Cu-sulfides by size fraction

3.2. Metallurgical performance

Table 3 presents the results from the reference tests conducted with the GTK cell, while Table 4 compiles the outcomes of all tests performed with the new Metso coarse particles flotation cell. The reference tests replicate the site operation using mechanical cells, where the site operates with a P80 of 180 µm and follows the reagent regimes described in Table 3. For the CPF cell, the P80 was set at 360 µm during testing. Although the same collector was used for both cells, a stronger frother was required for the CPF cell. Each of the tested technologies operates within distinct ranges for reagent dosage, Jg, and froth height. The reference tests highlight that the CPF cell, under its tailored conditions, is capable of achieving superior performance, even with a P80 twice as large as that used for the GTK cell.

The new CPF technology successfully discarded 41-43% of the mass fed into the circuit as final tailings in a single flotation stage, resulting in an overall copper recovery that was 5% higher than the conventional flotation process, despite using a P_{80} that was twice as large as that in the conventional flotation. The copper recovery exceeded 94% in the -150 µm fraction and surpassed 81% in the +150 µm fraction. Of the total tailings, 63% consist of particles coarser than 150 µm.

Table 3. Summary results: GTK

Run Order	P_{80} (µm)	Collector Dosage (g/Mg)	Frother (mg/dm³)	Mass Pull (%)	Cu Recovery Overall (%)
Ref Test 01	193	24	19	13.4	85.9
Ref Test 02	193	24	19	8.3	83.4

Table 4. Summary results: Metso's CPF Cell

Run Order	P_{80} (µm)	Collector (g/Mg)	Frother (mg/dm³)	Froth Level (mm)	Jg (cm/s)	Mass of feed to final tailings (%)	Cu Recovery Overall (%)	Cu Recovery +150 µm (%)	Cu Recovery - 150 µm (%)
1	360	20	20	250	2	66.1	73.9	57.4	86.0
2	360	20	20	100	1	87.1	68.2	55.0	76.5
3	360	20	40	250	1	75.3	75.2	60.0	85.5
4	360	20	40	100	2	54.8	79.0	61.7	91.4
5	360	40	20	250	1	74.2	78.9	69.8	85.2
6	360	40	40	250	2	56.7	82.4	72.5	89.4
7	360	40	40	100	1	83.2	71.1	60.4	78.4
8	360	40	20	100	2	69.0	64.0	54.0	70.6
9	360	40	40	250	2	56.8	84.3	73.0	92.7
10	360	40	40	400	2	43.5	89.0	81.1	94.5
11	360	40	40	400	2	41.1	89.6	81.9	94.8

3.3. Half factorial tests

The objective of the factorial tests was to identify which variables had the greatest impact on achieving high copper recovery with low mass pull. Minitab (version 18) was employed as the statistical tool to assess the influence of collector dosage, frother dosage, froth height, and air flowrate in relation to the response variables, including overall mass recovery, copper recovery, as well as mass and copper recovery in the +150 µm and -150 µm fractions.

Fig. 6 illustrates the probability plot for mass pull, and Fig. 7 for Cu recovery, where Minitab evaluates the data set through the Anderson-Darling test. The null hypothesis for this test assumes that the distribution follows a normal pattern. The sample population was 8.

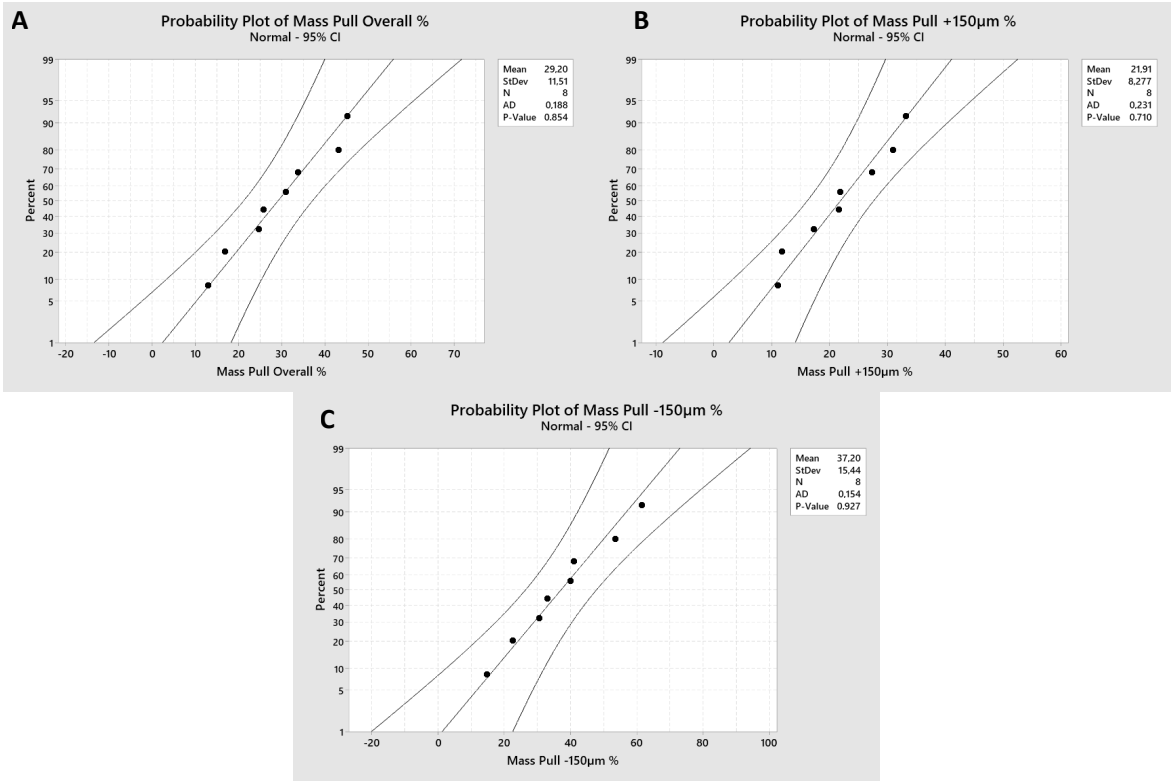

Fig. 6. Probability plot for mass pull – (A) Overall (B) +150 µm (C) -150 µm

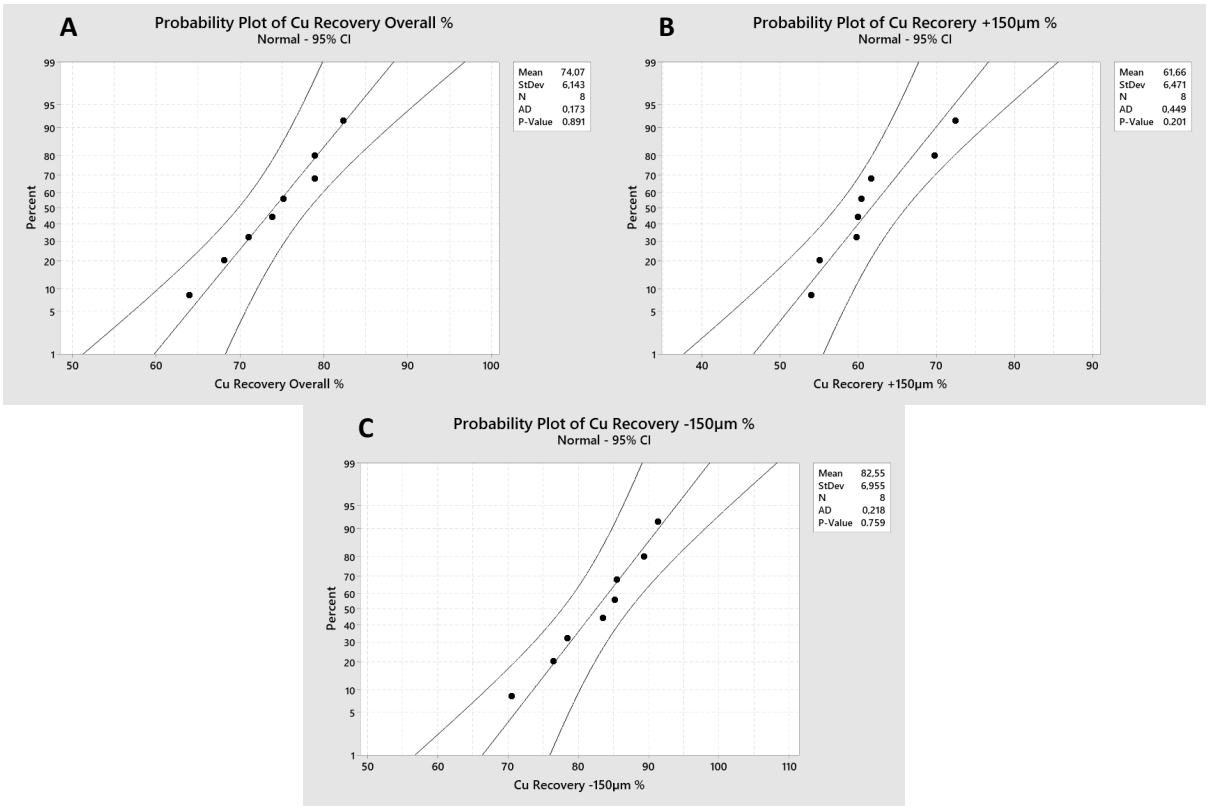

Fig. 7. Probability plot for Cu recovery – (A) Overall (B) +150 µm (C) -150 µm

The observed data align closely with the fitted distribution line, reinforcing the assumption of normality:

- Both the overall mass pull and overall Cu recovery data sets exhibit p-values (0.854 and 0.891, respectively) exceeding the conventional significance threshold of 0.05. This suggests that the null hypothesis, which posits that the data follow a normal distribution, cannot be rejected for either data set. Consequently, both data sets can be considered normally distributed. The mean mass pull was 29.2%, with a standard deviation of 11.5%, while the mean Cu recovery was 74.1%, with a standard deviation of 6.1%.
- The probability plots for mass recovery and Cu recovery in the +150 µm show a p-value of also above the 0.05 significance level (0.71 and 0.201, respectively), reinforcing the normality assumption. The mean mass pull was 21.9%, with a standard deviation of 8.3%, while the mean Cu recovery was 61.7%, with a standard deviation of 6.4%.
- The probability plots for both the mass pull and Cu recovery in the -150 µm fraction display p-values of 0.927 and 0.759, respectively, both exceeding the 0.05 significance threshold. This suggests that the null hypothesis that the data follow a normal distribution cannot be rejected for either dataset. Therefore, both datasets can be considered to be normally distributed. The mean mass pull was 37.2%, with a standard deviation of 15.4%, while the mean Cu recovery was 82.5%, with a standard deviation of 6.9%.

Figs. 8 and 9 illustrate the effects of variables on mass pull and Cu recovery, respectively.

Under the tested conditions, the process variables influenced both mass pull and copper (Cu) recovery in distinct ways. Jg was the most influential factor for mass pull across all size fractions, with higher values leading to greater mass pull. However, in terms of Cu recovery, Jg had a more limited effect, primarily benefiting the fine particle fraction.

Froth level and frother dosage played significant roles in Cu recovery across all fractions. For mass pull, froth level was especially important for coarse particles (+150 µm), while frother dosage had a stronger influence on fine particles (–150 µm).

Collector dosage showed no significant impact on mass pull in any size fraction, but it did affect Cu recovery differently depending on particle size, enhancing recovery for coarse particles, while decreasing it for finer ones.

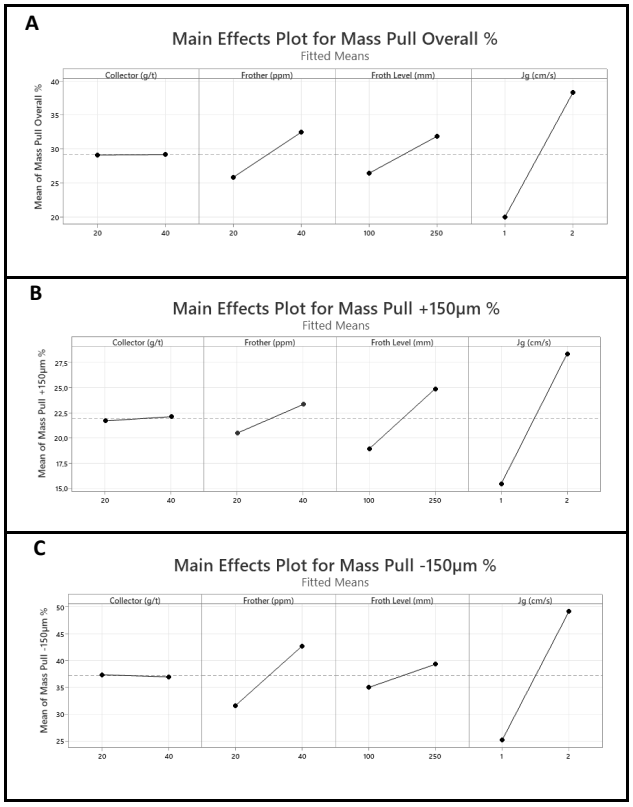

Fig. 8. Main effects plot for mass pull – (A) Overall (B) +150 µm (C) -150 µm

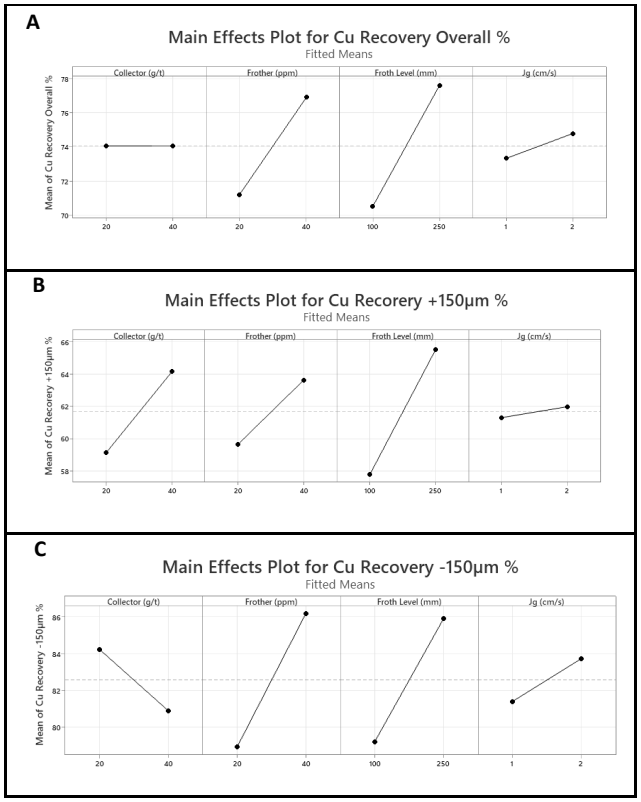

Fig. 9. Main effects plot for Cu recovery – (A) Overall (B) +150 µm (C) -150 µm

3.4. Comparison of the tested variable effects: froth feeding cells vs conventional flotation cells vs fluidized bed cells

Although the key process variables in froth-fed flotation cells are consistent with those used in conventional flotation systems, their influence on recovery, mass pull, and selectivity differs significantly due to variations in cell hydrodynamics and particle–bubble interaction mechanisms. Table 5 presents a comparative analysis of the effects of collector dosage, frother dosage, froth level, and superficial gas velocity (Jg) across froth-fed flotation, conventional mechanical flotation, and fluidized-bed systems.

Table 5. Comparison of the effects of key process variables in different flotation cells

Variable	Froth-fed flotation	Mechanical cells and columns flotation	Fluidized-bed systems
Collector dosage	Increasing collector dosage has a pronounced positive effect on the recovery of coarse particles; however, excessive dosage negatively impacts the recovery of fine particles. Among the evaluated process variables, collector dosage exhibited the least influence on overall mass pull.	Increasing collector dosage enhances coarse particles recovery and grades (Vianna et al., 2003; Hadler et al., 2005).	Collector dosage significantly influences recovery in fluidized-bed flotation systems. Increasing collector concentration reduces the extent of particle drop-back, thereby enhancing overall recovery (Moreno et al., 2016). However, excessive collector dosages can destabilize the froth phase, negatively impacting the recovery of coarse particles (Rahman et al., 2012). Unlike conventional flotation, fluidized-bed systems can achieve flotation at lower contact angles, thus requiring lower collector concentrations to achieve effective separation (Awatey, 2014). It should be noted that fines are generally removed prior to feeding fluidized bed units, so their effect is not determined.
Frother dosage	Frother dosage plays a critical role in froth stability and recovery across the particle size fractions. Increased frother concentration significantly enhances both recovery and mass pull. However, excessive dosages may reduce selectivity by promoting entrainment of gangue material. Thus, careful optimization is required to achieve high recoveries for coarse and fine particles while avoiding excessive mass pull.	Frother dosage plays a vital role in maintaining froth stability and ensuring selective separation. Higher frother concentrations typically improve recovery by enhancing froth persistence and reducing bubble coalescence (Ata, 2012; Huang et al., 2019).	Fluidized-bed flotation systems typically exhibit lower sensitivity to frother dosage. In configurations lacking a stable froth layer, frother is introduced at low concentrations via the fluidization water or air stream, primarily to aid fine bubble generation (Awatey, 2014). However, when a froth layer is present, frother dosage must be carefully regulated to maintain froth stability and enhance separation selectivity.
Froth level	Froth level has a significant influence on recovery, mass pull, and selectivity. Deep froth will result in higher recovery, higher mass pull, and lower selectivity. Specifically, with the coarse particles, the deep froth increases the probability of having the particle collected in the overflow.	In conventional flotation, increased froth depth enhances selectivity by allowing more time for water and entrained gangue to drain into the pulp, reducing non-selective recovery (Ata, 2012). However, greater froth depth can also increase particle drop-back (Yianatos	In fluidized-bed flotation cells, the froth zone is minimal or nearly absent due to the upward flow of fluidization water, which prevents stable froth formation. This allows coarse bubble-particle aggregates to rise without the buoyancy limitations seen in conventional flotation cells, where deep froth layers hinder coarse particle

		et al., 1998). Despite this, extended froth residence time generally improves mineral recovery by promoting sustained attachment of bubble–particle aggregates (Yianatos et al., 1998). Froth depth also correlates positively with air recovery, a strong predictor of flotation performance. High air recovery often corresponds with increased mineral recovery, though it may reduce mass pull (Hadler et al., 2012).	transport. As a result, FBFCs improve coarse particle recovery by enabling continuous overflow and enhancing bubble-particle interaction through hindered settling rather than relying on froth stability (Kromah et al., 2022).
Superficial gas velocity (Jg)	An increase in superficial gas velocity (Jg) influences both recovery and mass pull; however, it has the strongest impact on mass pull, suggesting that excessive air rates promote gangue entrainment and adversely affect selectivity.	Superficial gas velocity (Jg) significantly affects both recovery and mass pull. An increase in Jg decreases the residence time of bubble–particle aggregates in the froth, thereby reducing detachment and enhancing recovery. However, it also promotes water and gangue entrainment, which can lower concentrate grade (Yianatos et al., 1998).	Lower superficial gas velocity (Jg) is generally favorable for higher recovery in fluidized-bed systems, as low turbulence minimizes bubble–particle detachment (Fosu et al., 2015). However, increasing Jg can enhance coarse particle recovery up to an optimal threshold (Rahman et al., 2012). Beyond this point, particle drop-back increases with rising Jg (Moreno et al., 2016). Additionally, while bed level tends to decrease with increasing gas rate with possible loss in recovery, this effect diminishes with coarser bed particle sizes (Dankwah et al., 2022).

3.5. Repeatability tests

Following the initial half-factorial design experiments, Test 6 yielded the highest copper recovery. To confirm the reliability of this result, the test was repeated under the same operating conditions (Test 9). In addition, a new test condition (Test 10) was introduced to enhance copper recovery in the coarse particle fraction by increasing the froth level to 400 mm. This condition was also replicated (Test 11).

The results of these confirmatory and exploratory tests are summarized in Table 6.

Table 6. Summary results: Metso's CPF Cell repeatability tests

Run Order	Collector (g/Mg)	Frother (mg/dm³)	Froth Level (mm)	Jg (cm/s)	Mass of feed to final tailings (%)	Cu Recovery Overall (%)	Cu Recovery +150 μm (%)	Cu Recovery -150 μm (%)
	40	40	250	2	56.7	82.4	72.5	89.4
9	40	40	250	2	56.8	84.3	73.0	92.7
10	40	40	400	2	43.5	89.0	81.1	94.5
11	40	40	400	2	41.1	89.6	81.9	94.8

The results confirm the good repeatability of the baseline condition and highlight that increasing the froth level can enhance Cu recovery in both coarse and fine fractions; however, it also increases the mass pull, reducing the % mass of feed to final tailings. Tests 6 and 9 were conducted under identical baseline

conditions (collector dosage: 40 g/Mg, frother dosage: 40 mg/dm^3, froth level: 250 mm, and Jg: 2 cm/s) to assess repeatability. The results demonstrate high consistency, with nearly identical mass rejection to final tailings (56.7% in Test 6 and 56.8% in Test 9). Overall Cu recovery was slightly higher in Test 9 (84.3%) compared to Test 6 (82.4%). This improvement was more pronounced in the fine particle fraction, where Cu recovery increased from 89.4% to 92.7%. The coarse particle fraction (+150 μm) showed a modest increase from 72.5% to 73.0%. To explore the effect of a higher froth level, tests 10 and 11 were carried out using the same reagent dosages and Jg, but with an increased froth level of 400 mm. This adjustment resulted in a significant reduction in the mass of feed to final tailings (43.5% in Test 10 and 41.1% in Test 11). Both tests achieved higher overall Cu recoveries (89.0% and 89.6%, respectively). Recovery in the coarse particle fraction increased substantially to 81.1% and 81.9%, while fine particle recovery also improved to 94.5% and 94.8%, respectively.

The results also highlight the applicability of the froth-fed CPF cell as an early-stage gangue rejection device. By rejecting more than 40% of the feed mass as final tailings, the technology demonstrates its ability to remove a substantial proportion of coarse barren material without requiring this fraction to be ground to full liberation. Such pre-concentration not only reduces the load on downstream grinding and flotation circuits but also suggests potential savings in energy and reagent consumption.

3.6. Application within a copper processing flowsheet – grinding circuit

The results presented pertain to the application of the Coarse Particle Flotation (CPF) cell within the grinding circuit, positioned upstream of the final grinding stage preceding conventional flotation. Figs. 10 and 11 illustrate the grinding circuit configurations without and with the integration of the novel CPF cell, respectively.

Fig. 10 illustrates the conventional grinding circuit configuration prior to the integration of coarse particle flotation. Material balance data indicate that the flotation feed has a P_{80} of 193 μm with a copper grade of 0.83% and 100% solids recovery at 100 Mg/h. This configuration represents the baseline condition for comparison with flowsheets that include the CPF cell for early coarse particle recovery.

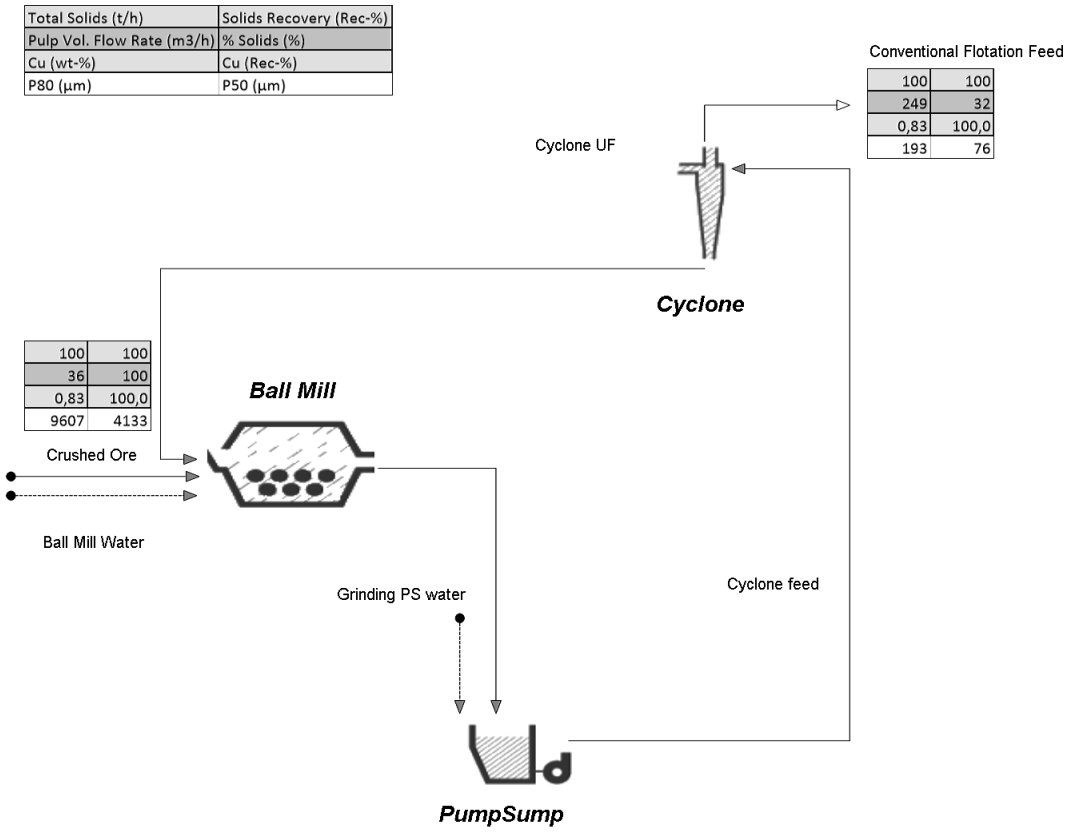

Fig. 10. Example of a conventional grinding circuit in copper plants

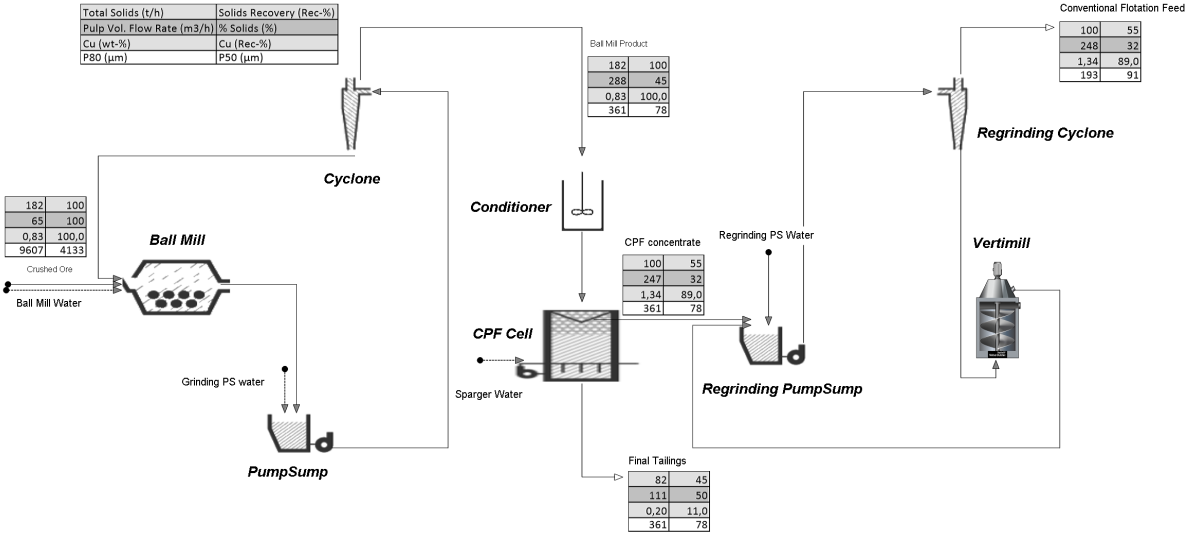

Fig. 11. Grinding circuit with the integration of the CPF cell

The integration of the Coarse Particle Flotation (CPF) cell enables a two-stage grinding process, with the CPF cell positioned between the stages (Fig. 11). In the first stage, the entire plant throughput is ground to a P_{80} of approximately 360 µm. Only the CPF concentrate proceeds to the second grinding stage, where it is further reduced to a P_{80} of 193 µm, the target size for conventional flotation.

The CPF circuit is simple and compact, comprising a conditioning tank and the CPF cell. The optimal configuration places the conditioning tank directly above the cell to allow gravity-fed operation. Auxiliary equipment includes pumps for delivering water to the spargers and transporting the products. The conditioning tank serves both to mix reagents and stabilize the feed flow to the CPF cell.

Unlike conventional or fluidized-bed systems, the CPF cell employs a froth-fed design that eliminates the need for feed classification. In fact, to maximize plant capacity, classification ahead of the CPF cell should be avoided. The upstream mill can also serve as the reagent conditioning zone.

The CPF cell is capable of operating with feed slurry concentrations ranging from 40% to 65% solids (w/w). In the configuration shown in Fig. 11, the CPF cell is operated at 45% solids, producing a concentrate at 32% solids and tailings at 50% solids. These slurry characteristics allow for material handling practices similar to those used in conventional flotation circuits. The CPF concentrate requires no dewatering and is sent directly to the regrinding classification circuit to achieve the desired particle size for conventional flotation.

The CPF tailings stream, which includes both fine and coarse particles, constitutes the final tailings. In the tested configuration, the CPF circuit rejected 45% of the total plant feed mass while recovering 89% of the copper content. As a result, the conventional flotation circuit continues to process 100 Mg/h of solids, but with an upgraded copper grade of 1.23%. In the baseline circuit (Fig. 9), only 0.83 Mg/h of copper entered conventional flotation; following CPF integration, this increased to 1.23 Mg/h—representing a 47% gain in copper tonnage without expanding the flotation circuit.

Furthermore, by rejecting 45% of the feed mass in the CPF stage, total plant capacity increased from 100 Mg/h to 182 Mg/h—an 82% increase. Although the grinding circuit would require resizing to accommodate this higher throughput, the conventional flotation circuit remains unchanged and could potentially operate at improved recoveries and concentrate grades. This suggests potential savings in energy and reagents and improved circuit efficiency. While promising for early gangue rejection in existing plants, further pilot- and plant-scale studies are needed to confirm industrial feasibility and economic viability.

4. Conclusions

This study presented the development and initial evaluation of a novel coarse flotation technology that uses the froth feeding principle. The technology demonstrated several operational advantages, including the elimination of fluidization (resulting in reduced water consumption), the ability to handle

concentrate with solid contents comparable to conventional flotation, and the treatment of the full particle size distribution without the need for pre-classification.

A half-factorial Design of Experiments (DoE) was used to assess the effects of key process variables on separation performance. The results showed that froth level, frother dosage, and superficial gas velocity (Jg) were the primary factors influencing copper recovery. Collector dosage exhibited contrasting effects: while beneficial for the recovery of coarse particles, it negatively impacted the recovery of fine particles. Among the controllable flotation cell parameters, froth level emerged as the most critical for maximizing Cu recovery. Although Jg maintained a positive effect, it was more strongly correlated with mass pull, indicating that minimizing Jg, while still achieving target recovery, can enhance selectivity by increasing tailings rejection.

Laboratory-scale experiments confirmed that the new technology is capable of achieving superior Cu recovery relative to conventional flotation, even when processing feed material with substantially coarser particle sizes. These findings suggest significant potential for improving both metallurgical performance and resource efficiency in flotation circuits.

The results indicate that the froth-fed CPF cell shows potential as a flotation device for early gangue rejection; however, pilot and plant-scale testing are needed to confirm industrial feasibility. When applied upstream of conventional flotation, it could increase the feed grade from 0.83% Cu to 1.23% Cu while rejecting over 40% of the mass as final tailings, without requiring this fraction to be ground to full liberation. These outcomes suggest possible reductions in grinding energy and reagent demand, which may improve overall circuit efficiency.

Acknowledgments

The authors gratefully acknowledge Metso for providing project funding, as well as all team members from various departments involved in the design of the new technology and those who contributed to the execution of the laboratory tests and sample preparation. Part of this paper was presented at XXXI International Mineral Processing Congress 2024 / Washington, DC / Sep 29–Oct 3. The journal version includes several important updates and enhancements compared to the original conference paper. The authors also used ChatGPT (OpenAI) to assist with language editing; all scientific content, analyses, and conclusions remain the sole responsibility of the authors.

References

ASLAN, N., ABBAKER, A., 2023. *The effect of microbubbles on coarse particle anionic flotation: analysis and optimization*. Physicochemical Problems of Mineral Processing, 59, 6.

ANZOOM, J.S., BOURNIVAL, G., ATA, S., 2024. *Coarse particle flotation: A review*. Minerals Engineering, 206.

ATA, S., 2012. *Phenomena in the froth phase of flotation – A review.* International Journal of Mineral Processing, 102–103, 1–12, https://doi.org/10.1016/j.minpro.2011.09.008.

AWATEY, B., THANASEKARAN, A., KOHMUENCH, J.N., SKINNER, W., ZANIN, M., 2014. *Critical contact angle for coarse sphalerite flotation in a fluidised-bed.* Minerals Engineering, 60, 51–59.

AWATEY, B., SKINNER, W., ZANIN, M., 2015. *Incorporating fluidized-bed flotation into a conventional flotation flowsheet: A focus on energy implications of coarse particle recovery*. Powder Technology, 275, 85-93.

CARVALHO, M., SHERRELL, I., BAYARMAGNAI, E., 2025. *Slurry feeding arrangement*. US20250018404A1.

CLARK, M.E., BRAKE, I., HULS, B.J., SMITH, B.E., YU, M., 2006. *Creating value through application of flotation science and technology*. Minerals Engineering, 19, 6-9, 758-765.

DANKWAH, J., ASAMOAH, R., ZANIN, M., SKINNER, W., 2022. *Influence of water rate, gas rate, and bed particle size on bed-level and coarse particle flotation performance*. Minerals Engineering, 183.

FORBES, L., BRILL, C., VERSTER, I., FRANKS, G.V., 2025. *Novel reagent addition method for improved copper recovery*. Cleaner Engineering and Technology 26.

FOSU, S., AWATEY, B., SKINNER, W., ZANIN, M., 2015. *Flotation of coarse composite particles in mechanical cell vs. the fluidised-bed separator (The Hydrofloat™)*. Minerals Engineering, 77, 137–149.

HADLER, K., AKTAS, Z., CILLIERS, J.J., 2005. *The effects of frother and collector distribution on flotation performance.* Minerals Engineering, 18, 2, 171-177.

HADLER, K., GREYLING, M., PLINT, N., CILLIERS, J.J., 2012. *The effect of froth depth on air recovery and flotation performance*. Minerals Engineering, 36-38, 248-253.

HASSANZADEH, A., SAFARI, M., HOANG, D.H., KHOSHDAST, H., ALBIJANIC, B., KOWALCZUK, P.B., 2022. *Technological assessments on recent developments in fine and coarse particle flotation systems*. Minerals Engineering, 180.

HUANG, Q., YANG, X., HONAKER, R.Q., 2019. *Evaluation of frother types for improved flotation recovery and selectivity*. Minerals, 9-10, 590.

JAMESON, G.J., 2007. *Method and apparatus for flotation in a fluidized bed*. PCT Patent 200810422A1, September 4, 2008.

JAMESON, G.J., 2010. *New directions in flotation machine design*. Minerals Engineering, 23, 835-841.

JAQUES, E., VOLLERT, L., AKERSTROM, B., SEAMAN, B.A., 2021. *Commissioning of the coarse ore flotation circuit at Cadia Valley Operations – challenges and successes*. Mill Operators Conference, 2021, 124-138.

KNAUS, O.M., 1968. *Verfahren zur flotation von mineralien und vorrichtung zur durchfuhrung des verfahrens*. DE Patent No 1,257,704, 4 Jan. 1968.

KOHMUENCH, J., MANKOSA, M., THANASEKARAN, H., HOBERT, A. 2018. *Improving coarse particle flotation using the HydroFloat™ (raising the trunk of the elephant curve)*. Minerals Engineering, 121, 137-145.

KROMAH, V., POWOE, S.B., KHOSRAVI, R., NEISIANI, A., CHELGANI, S.C., 2022. *Coarse particle separation by fluidized-bed flotation: A comprehensive review*. Powder Technology, 409.

LEPPINEN, J.O., LASHKUL, A.V., NENNO, V.E., INGERTTILÄ, K.T., KALLIOINEN, J.O., 2003. Separation in Froth – An effective technique for coarse flotation. International Mineral Processing Congress, Cape Town, South Africa, 882-892, ISBN:0-958-46092-2.

MANKOSA, M.J., LUTTRELL, G.H., 2002. *Air-assisted density separator device and method*. U.S Patent 6,425,485, July 30, 2002.

MORENO Y.S., ATA, S., 2016. *On the detachment of hydrophobic particles from the froth phase.* Minerals Engineering, 95, 113-115.

MUDD, G.M., 2009. *The Sustainability of Mining in Australia: Key Production Trends and Their Environmental Implications for the Future*. Department of Civil Engineering, Monash University, ISBN: 978-0-9803199-4-1.

NENNO, V.E., LASHKUL, A.V., LEPPINEN, J.O., BJORKLOF, S.V., 2004. *Apparatus for separation of solids in froth*. U.S Patent, 6,776,292, August 17, 2004.

RAHMAN, R.M., ATA, S., JAMESON, G.J., 2012. *The effect of flotation variables on the recovery of different particle size fractions in the froth and the pulp*. International Journal of Mineral Processing, 106–109, 70-77.

ROSS, V.E., 1993. *Separation Method and Apparatus*. SA Patent No. 93/5367.

RÖTZER, N., SCHMIDT, M., 2020. *Historical, Current, and Future Energy Demand from Global Copper Production and Its Impact on Climate Change*. Resources, 9, 4, 44, https://doi.org/10.3390/resources9040044.

TOLLANDER, E., CARVALHO, M., JUVONEN, T., 2025 *Gasified fluid supply arrangement and flotation cell*, WO2025017244A1.

TRAHAR W.J., WARREN L.J., 1976. *The floatability of very fine particles – A review*. International Journal of Mineral Processing, 3, 103-131.

URIZAR., D., 2011. *Procedure and apparatus of the concentration of hydrophobic materials*. U.S. Patent No 8,038,012, 18 Oct. 2011.

VIANNA, S.M., FRANZIDIS, J., MANLAPIG, E.V., SILVESTER, E., FU, P., 2003. *The influence of particle size and collector coverage of the floatability of galena particles in a natural ore*. 22nd International Mineral Processing Congress, Cape Town, South Africa, 816-826.

WANG, G., NGUYEN, A.V., MITRA, S., JOSHI, J., JAMESON, G.J., EVANS, G.M., 2016. *A review of the mechanisms and models of bubble-particle detachment in froth flotation*. Separation and Purification Technology, 170, 155-172.

YIANATOS, J.B., BERGH, L.G., CORTÉS, G.A., 1998. *Froth zone modelling of an industrial flotation column*. Minerals Engineering, 11(5), 423-435.